Degradations analysis and aging modeling for health assessment and prognostics of PEMFC

Marine Jouin*, Rafael Gouriveau, Daniel Hissel, Marie-Cécile Péra, Noureddine Zerhouni

FEMTO-ST Institute, UMR CNRS 6174 - UBFC / UFC / ENSMM / UTBM,
FC-LAB Research, FR CNRS 3539,
24 rue Alain Savary, 25000 Besançon, France
firstname.lastname@femto-st.fr

Abstract

Applying prognostics to Proton Exchange Membrane Fuel Cell (PEMFC) stacks is a good solution to help taking actions extending their lifetime. However, it requires a great understanding of the degradation mechanisms and failures occurring within the stack. This task is not simple when applied to a PEMFC due to the different levels (stack - cells - components), the different scales and the multiple causes that lead to degradation. To overcome this problem, this work proposes a methodology dedicated to the setting of a framework and a modeling of the aging for prognostics. This methodology is based on a deep literature review and degradation analysis of PEMFC stacks. This analysis allows defining a proper vocabulary dedicated to PEMFC's prognostics and health management and a clear limited framework to perform prognostics. Then the degradations review is used to select critical components within the stack, and to define their critical failure mechanisms thanks the proposal of new fault trees. The impact of these critical components and mechanisms on the power loss during aging is included to the model for prognostics. This model is finally validated on four datasets with different mission profiles for health assessment.

Keywords: Proton exchange membrane (PEM) fuel cell, Health assessment, Prognostics, Critical components, Aging model

1. Introduction

Considered as a promising technology for chemical energy conversion into electricity, Proton Exchange Membrane Fuel Cells (PEMFC) are no more far from a large scale deployment. However, some improvements are still required to extend the lifetime of these systems. Prognostics and Health Management (PHM) appears as a great solution to help tackling this issue. Indeed, PHM is composed of a set of activities starting from monitoring and data processing. This leads to health assessment, diagnostic and prognostics, to finally use all the gathered information for decision making. This whole proposition aims at taking the right decisions at the right time to help preserving a system and extending its lifetime until its mission is complete. PHM of PEMFC is still a very recent research topic and a lot of challenges can be highlighted, particularly regarding prognostics [1].

Prognostics can be considered as the key process of PHM at it enables predicting the future behavior of a system as well as its remaining useful life (RUL) [2]. Prognostics applications on PEMFC are still rare in literature but are developing. Different approaches can be identified: 1) data-driven approaches [3, 4, 5], and 2) model-based or hybrid approaches [6, 7, 8]. However, they do not include explicitly the mission profile making their applications limited.

To support PHM, failure analysis and reliability modeling of PEMFC should be developed. Different dependability analyses are already existing regarding PEMFCs such as [9, 10] if the whole system is considered. As the stack is the major concern of this work, let's go down to that level. Some interesting works focusing on failure and dependability analysis of PEMFC stacks can be found in literature: fault tree analysis [11, 12, 13], Petri nets [14] or other classifications created for the needs of the authors [15, 16]. The major drawback of these works is the lack of explicit hypotheses preventing to know in which context these studies can be used. It is widely asserted that PEMFC are reliable systems as they do not have any moving part. Nevertheless, numerous degradation mechanisms tend to shorten their lifetime.

To built a degradation model suitable for health assessment and prognostics, a great understanding of all the aging mechanisms occurring within a PEMFC stack is needed. Current reviews on PEMFC degradations [15, 17, 18, 19] are becoming too old, new experiments and understandings have appeared since then.

This paper aims at developing a degradation and fail-

*Corresponding author, Tel.: +33 (0)3 81 40 27 96, Fax +33 (0)3 81 40 28 09

ure analysis dedicated to PHM and more precisely to heatlth assessment and prognostics of PEMFC stacks. Indeed, with this focus, a deep understanding of degradation will help selecting critical components which degradation strongly impact the outputs of the stack, namely the power and the lifetime. Once these critical components selected, the main aging mechanisms are chosen and their impact is integrated in a degradation model that can be used for prognostics. The main contributions of this work are:

1. the proposal of a standardized vocabulary for PHM of PEMFC;
2. the definition of a working framework for reliability analysis and PHM of PEMFC;
3. a new degradation and failure analysis based on an updated literature review;
4. and based on this analysis, a new degradation model of the stack is proposed, analyzed and partially validated.

To achieve these goals, the paper is organized as follow. First, the background of PEMFC functioning is briefly reminded. This allows defining the vocabulary necessary for the study as well as a working framework for PHM. Section 3 is dedicated to the degradation and failure analysis, critical components are selected before choosing their main degradations that will appear in a degradation model. This is used in Section 4 to set a degradation model based on physics that includes both the aging and the current demand. Finally, the capabilities of the model for health assessment are demonstrated on four datasets in Section 5 before concluding.

2. Toward a prognostics working framework

2.1. Proton Exchange Membrane Fuel Cells

PEMFC is a specific fuel cell type using air (oxygen) and hydrogen to produce electricity, water and heat [20]. It can be encountered in a wide variety of applications [21] such as transportation (car, boats, etc.), stationary applications (auxiliary power unit, combined heat and power generation (μ-CHP)) or powering of portable devices, alone or combined with other devices like batteries or ultra-capacitors.
Different levels of system granularity exist. First, a "PEMFC system" refers to a PEMFC stack and all its auxiliaries (reactant storages, pumps, etc.). The stack is the part that converts the energy and is referred as the fuel cell. The stack is an assembly of elementary cells. Their number may vary from a single one to several hundreds depending of the output power expected from the stack. Finally, a cell is composed of different components (Fig. 1). To provide electricity, different oxydo-reduction reactions occur within the stack [7]. The global reaction equation of the system is:

$$H_2 + \frac{1}{2}O_2 \rightarrow H_2O + electricity + heat \qquad (1)$$

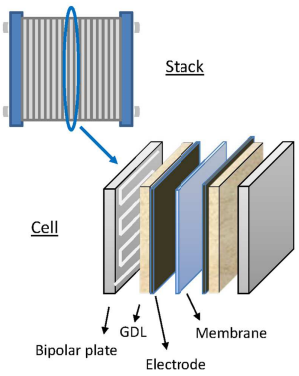

Figure 1: The different components of a PEMFC stack

Different output powers can be obtained from a stack. It depends on the input mission profile which can be expressed in terms of current (in Amperes) or power requirements (in Watts). In this work, the stack input is defined by the current whereas the power is the observed output. As it will be shown later, the mission profile strongly impacts the lifetime of the stack. To allow current variations the auxiliaries make the operating conditions varying (temperatures, pressures, etc.) to maintain the stack in its nominal operating conditions. If not, a degradation may happen. In this study, the focus is the stack and its subcomponents. The operating conditions are supposed always optimal and the auxiliaries never fail. In that way, a stack failure is only due to its own aging.
The vocabulary used in this work is now be defined.

2.2. Vocabulary definition

As fuel cell and reliability or PHM communities tend to use different vocabularies, it is important for a good understanding to define a precise vocabulary. Let's start with the terms "reversible degradation" and "irreversible degradation" used in a lot of PEMFC papers.

2.2.1. Degradation and reversible phenomena

During the aging of the stack, all the components age and their performance decreases. This can be seen in the power delivered by the stack particularly with a constant current profile where the power, instead of remaining constant, decreases slowly with time, Fig. 2. However, when the stack is stopped for a resting period or for characterizations, recoveries can be observed on the power. Indeed, some phenomena occurring during the aging are reversed, Fig. 2.

The existing expression, namely "reversible degradation", regarding these phenomena may sound weird out of the FC community. In that community, this expression is often opposed to "irreversible degradation". To use standardized vocabulary, the terms are re-defined according to the norm EN 13306 [22]. Degradation is defined as: "An irreversible process in one or more characteristics of an item

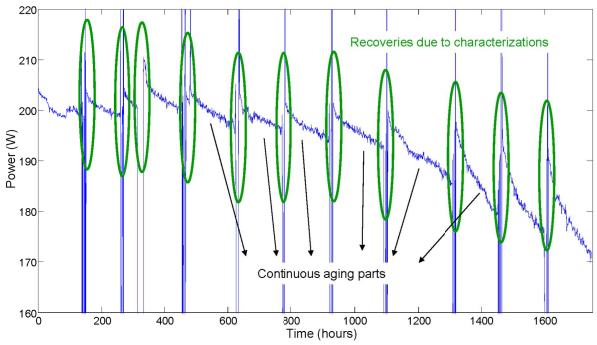

Figure 2: Evolution of the power delivered by stack of a 5 cells and 100cm2 active area, during 1750 hours under 60A. Illustration of the power recovery during the aging

with either time, use or an external cause". Consequently, the expression "irreversible degradation" is reduced to the word degradation. "Reversible degradation" is a nonsense regarding the norm definition. It is replaced by reversible phenomena or reversible mechanism.
Reversible phenomena have been observed in different works [23, 24] but are not fully explained. They appear in voltage and power measurements in forms of recoveries. Interruptions of continuous testing by resting periods, characterizations with *in-situ* methods or major changes in gas flows seem to be some causes of the phenomena. When the stack goes through changing operating conditions, gas and water diffusion within the cells are affected, changing their spatial distributions. These reversible phenomena are part of transient regimes and disappear once the stack comes back to a permanent regime.

2.2.2. Modes and failure

Then, in the PEMFC literature, the notion of mode is unclear. For example the expression "degradation mode" can be found referring to the appearance and evolution of a degradation. In this paper, we prefer using "degradation mechanism" or "failure mechanism" to deal the degradation's appearance and evolution. For this purpose, the reference is the standardized definition of degradations: "Physical, chemical or other processes which lead or have led to failure" [22].
Consequently, the word "mode" is kept for a different context. It refers to a functioning mode, for example to a healthy or degraded mode. A degraded mode is defined as "State of an item whereby that item continues to perform a function to acceptable limits but which are lower than the specified values or continues to perform only some of its required functions". When using this definition, a new question appears: what is a degraded mode for a PEMFC stack? Indeed, when no dramatic failure happens, the end of life of the stack is determined by the percentage loss of initial power [25]. So a degraded mode could be a certain percentage of power loss, but in which proportion? That might be a question to raise for future works.
As the vocabulary is now set, a working framework defining the context and hypotheses for PHM is described.

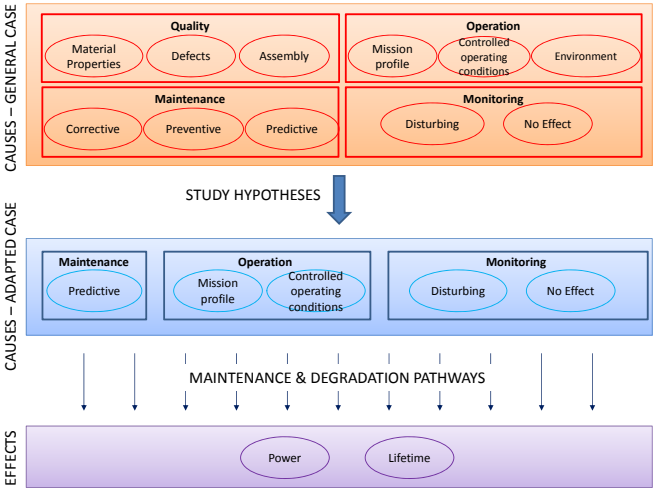

Figure 3: General framework for prognostics of a PEMFC stack - from causes to consequences

2.3. Working framework for PHM

To practice prognostics, and more generally PHM, it is necessary to have a good understanding of the system: its working conditions, its environment and all the other factors that influence its functioning. An attempt of architecture of the stack environment is proposed in [16]. It distinguishes the causes of failure coming from manufacturing from those coming from the stack utilization. Also it underlines three factors affected by performance loss: stability, power and lifetime. However, the vocabulary is globally unclear and the structure proposed in [16] does not meet the needs of this study, a new framework showing the different environmental factors around the stack and the characteristics impacted is proposed, Fig. 3. The objective is to propose a general working framework for PHM of PEMFC applications (upper part), and to reduce its scope according to hypotheses or specificities of real cases (middle part).

Whatever the use of the PEMFC stack, the two output parameters of interest are the power delivered and the lifetime. These parameters can vary positively or negatively in function of a certain number of causes divided into: (1) quality, (2) maintenance, (3) operation and (4) monitoring.
Regarding quality, its definition gathers the physical properties of the stack components, the manufacturing defaults as well as the characteristics of the assembly.
The maintenance part integrates corrective, predictive (in which PHM is included) and preventive maintenance. As no clear corrective or preventive maintenance strategies exist at the stack level [26], we assume that they could contain: stack reconstruction, sealing correction or removal of failed cells. Even if these kind of maintenance are not systematic yet, a large scale deployment of fuel cells may

change that.
The operation is defined by three items:

1. the mission profile, which is limited to the current demand and does not take into account disturbances introduced by measurements or by the re-calibration;
2. the operating conditions that can be controlled as the stack temperature, stoichiometries or reactant pressures, among others;
3. the environmental factors that cannot be controlled such as air pollution, vibrations or environment temperature.

Regarding monitoring, as not all the measurements made on the stack have a significant impact, two categories can be distinguished:

1. "disturbing" measures means creating disturbances in the stack behavior such as polarization curve measurements or electrochemical impedance spectrometry (EIS) which create power recovery phenomena, or as cyclic voltametry that needs a modification of the gas supplies;
2. "no effect" measures means that seem to have no impact on the stack behavior such as voltage, current measurements or other external measures (temperature, pressure, etc.) along the power supply.

According to the hypotheses introduced in this work, some causes can be ignored. This is illustrated on the middle layer of Fig. 3. The quality of the stack can influence the performance [23], but here it is considered as perfect so all the corresponding category is left apart. Maintenance is limited to predictive maintenance. And the experiments conducted in the lab are realized in a controlled environment: the influence of environment can be ignored.
The link between the causes and the effects is made by the maintenance and degradation pathways. Afterward, as predictive maintenance is limited to prognostics with no consequent decision making and action in this work, only degradation pathways will be considered. However it was important to show that the power and the lifetime can be positively or negatively impacted.
To go further in the analysis, a detailed knowledge of the degradation mechanisms within the stack is needed. The next section is dedicated to a literature review and analysis of aging and failure mechanisms in PEMFC.

3. Degradation, failure mechanisms and criticality analysis

This analysis aims now at classifying and analyzing the degradation mechanisms to exploit them for modeling. The main idea is to start from the stack's degradation and by different selection processes to go to a degradation model useful for health assessment and later for prognostics. First the degradation phenomena are reviewed, then the components are classified regarding their contribution to the loss of power of the stack during the aging and the most critical components are selected. For the selected components, it is interesting to choose the leading mechanisms as they cause the greatest loss of performance. They are finally used in a degradation model.

3.1. Scope of the analysis

3.1.1. Degradation levels

The major difficulty in the apprehension of the behavior and the aging of a PEMFC stack mainly lies in the different system's levels (stack-cell-component). And if one goes to the component level, micro and nano scales are rapidly reached. This variety of levels and scales to take into account is one of the major difficulty to built behavioral and/or degradation models suitable for prognostics. Moreover, many of the parameters used to describe small scale phenomena cannot be accessed easily.

3.1.2. Hypotheses and limits of the study

Some hypotheses are set to to limit the literature review to the essential degradation mechanisms according to our prognostics' goal and also to correspond to the operating conditions of the datasets introduced later.
First, it is assumed that, in cases of variable current profiles, the operating conditions are automatically regulated and set to their nominal values. The stack cannot suffer from fuel starvation. This limits the impact of non-nominal operating conditions, like out of range temperatures or humidities for example.
Then, start-up and shut-down of the system as well as extreme working temperatures are not considered. Moreover, only phenomena with characteristic times in hours are taken into account. Fast phenomena such as the drying of the membrane or cathode flooding are left aside.

3.2. Degradation phenomena

3.2.1. Bipolar plates

Structure and role. The bipolar plates are the skeleton of the stack. They isolate the individual cells, conduct the current between the cells, help in water and thermal managements but also provide flow fields for incoming reactants and outgoing products. The ideal characteristics for their material are among others : a high electronic conductivity, a great resistivity to corrosion, a strong mechanical resistance, low thermal and electrical contact resistances, a low permeability to reactant gases and no brittleness [19, 27].

Degradation description. The analysis of degradation of bipolar plates is still an open issue. According to [18, 19], three degradation mechanisms intervene: (1) corrosion leading to the production of multivalent cations that impact seriously the durability of the membrane and the catalyst layers; (2) appearance of a resistive surface layer on the plates leading to a higher ohmic resistance; and (3)

fractures or deformation of the plates accentuated by operational factors such as thermal cycles, bad temperature distributions or non-uniform currents.

Degradation modeling. No clear aging modeling can be found in the literature. However, [27] suggests that the behavior regarding corrosion can be obtained thanks to potentio-dynamic polarization curves of the materials.

3.2.2. Gas diffusion layers

Structure and role. The GDL, with its porous nature, plays an essential role for assisting the reactions of hydrogen oxidation and oxygen reduction in the catalyst layers by allowing the reactant to diffuse from the flow fields to the active sites. It facilitates water management in the catalyst layer and in the membrane by ensuring the diffusion of vapor water mixed with the reactants and by evacuating liquid water out of the stack. The GDLs are electrically conductive to ensure the electrons transfer from the catalyst layer to the bipolar plates [28]. Porous GDLs are typically composed of a microporous layer (MPL) and a gas diffusion backing (GDB). The MPL with the good pore structure and hydrophobicity is essential for reducing the contact resistance and for removing water from the catalyst layer. GDLs are used under a strong pressure constraint (> 100 psi) so the materials have to meet different requirements regarding electric and plastic deformations or gas permeability. Reactant go through the GDL both by convection and diffusion.

Degradation description. Because of the major difficulty of separating the degradation of the GDL from that of the membrane-electrodes assembly, most of the aging studies on GDL are *ex-situ*. Three main changes can be observed when the GDL degrades: (1) behavior modifications regarding water due to the loss of hydrophobicity and changing of the carbon surface; (2) changes in the GDL structure due to the carbon corrosion and the mechanical constraints; and (3) changes in the electrical and thermal resistances combined with a loss of porosity.
Polarization curves proposed in [29] indicate that the GDL degradation has more impact on the stack performance when high current densities are concerned.

Degradation modeling. Existing models for GDL are mostly behavioral model on gas diffusion and mass transports in the stack. Models for performance losses during the aging and temporal evolution of diffusion parameters are scarce. [30] proposes an approach combining two modeling methods linking the stack's performance loss to the loss of hydrophobicity.

3.2.3. Electrodes

Structure and role. The electrodes are composed of two layers: a catalyst layer and a support for that layer, the carbon support. A conventional catalyst layer is made with platinum (Pt) nanoparticles supported by a surface of black carbon in close contact with a controlled quantity of ionomer (membrane material). The carbon support allows the nanoparticles to have a high dispersion (2-3 nm) and provides a porous structure electronically conductive. This structure plays a crucial role in reactants and electrons transports to the nanoparticles as for evacuating gases and water. The ionomer maintains discrete hydrophilic and hydrophobic domains for the reactants and protons accesses to the active sites for the Pt nanoparticles [31]. According to [18], the impact of the degradation is not the same for both electrodes (anode at the hydrogen input or cathode at the oxygen side).

Degradation description. Two main families of phenomena are responsible of the loss of performance with the electrodes: the catalyst layer degradation [31, 32] and the carbon support degradation [19, 31]. Together these phenomena lead to a loss of active area of the electrode and its consequent loss of electrochemical activity. Among them, we can find: (1) the dissolution and diffusion of Pt through the ionomer, re-deposit on other particles forming bigger particles or diffusion through the membrane to create a band; (2) the carbon corrosion into dioxide and consequent disintegration of the catalytic layer leading to Pt agglomeration and to the formation of oxides on the carbon surface; (3) the generation of reactive species as the hydrogen peroxide (H_2O_2), radicals of hydroperoxyl ($^{\bullet}OOH$) and radicals $^{\bullet}OH$ causing the degradation of the membrane; and (4) reversible and irreversible adsportion of contaminants from air, reactants or products from other components degradation.
The anode remains almost unaffected by the dissolution, oxidation and agglomeration of Pt, whatever the conditions. By contrast, the cathode is very impacted and this results in a loss of active area in time [18]. It is aggravated by potential and temperature cycles.
The durability of the electrodes is strongly impacted by the operating condition of the stack. According to a research team from Nissan, in light vehicle applications, the degradation rates of the electrodes can be divided into three categories [31]: idling, representing 28% of the time in the stack lifetime; start/stop cycles, 28% and load cycling, 44%.
Let's start with the idling. When a functioning vehicle stops, for example at a stoplight, the stack has to keep on providing a minimum power to supply to the auxiliaries. In that case, the required current is very low which corresponds to a high potential in each cell of the stack (near open circuit voltage (OCV) conditions), around 0.9 - 0.95 V. This creates a favorable environment for the reactions of Pt degradation. Representing the same percentage as the idling, there are the start/stop cycles. They have a serious impact on the carbon support corrosion [33].
Finally, the load cycling represents the major part of the stack lifetime in automotive but also in the other applications. They model mission profiles with durations at low or high potentials and ramp transitions. For a given cycled

profile, the degradation is higher (by time unit) than for a constant current for the same range and same duration [31]. It shows a significant contribution in the degradation of the increasing and decreasing ramps during current transitions.
The impact of contamination can also be mentioned. After hundreds of hours, its impact become an important factor in performance loss. Indeed, black carbon surfaces play roles of filters and absorb easily the impurities. The Pt is sensitive to the adsorption of contaminants such as CO, SO_2, H_2S, NO_2, NO and NH_3 that occupy the active sites in a reversible or irreversible manner.

Degradation modeling. Modeling all the phenomena influencing the electrodes degradation can be really complicated and it is interesting to model them separately. It is on this basic idea that the authors in [34] model what they call the fingerprint of the carbon degradation. Their results show that the performance loss of the PEMFC (P) can be linked to the loss of carbon (p_C)during the aging by an exponential law: $P = a.exp(b.p_C)$.
In [35], three reactions related to Pt dissolution and oxides reactions are taken into account: the Pt dissolution (r_1), the formation an oxide film (r_2) and the dissolution of the oxide film (r_3). The model results are coherent with author data and this model serves as a basis for several other works on electrode degradation. One of them deals with a modeling for the decreasing of the active area for prognostics purpose [6]. The exponential decreasing obtained in the paper is coherent with observations reported in [17, 19, 36]. Other models coupling several phenomena can be found in [37, 38]. Finally, a model expressing the loss of active area as a function of the number of potential cycles is proposed in [39].

3.2.4. Membrane
Structure and role. Membranes used in PEMFC are ionomers, i.e. polymers modified to include ions, usually sulfonic groups. The ionic hydrophilic portions are key elements to allow protons transport through the membrane. Among different types of membranes [40, 41], the most used is based on perfluorosulfonic acid (PFSA) such as the Nafion. As it is the type used for experiments, the emphasis is put only on this type. To fulfill their function, when the membrane absorbs water, ionic domains swell and create conductive channels for protons. The proton conductivity raises with the water content, until a limiting value.
The membrane has several roles in the cell. First, it allows the protons transport from the anode to the cathode thanks to its hydrophilic and hydrophobic domains. Then, it acts as a separation between the fuel and the air. A membrane has to have an excellent proton conductivity, a thermal and chemical stability, a good mechanical resistance, flexibility, a low permeability to gases and a low water drag. According to [40], usually the life duration of the membrane determines the lifetime of the PEMFC.

Degradation description. To consider the membrane's degradation, [42] proposes three categories:

1. Chemical degradation: direct attacks of the polymer by radical species leading to the decomposition of the membrane;
2. Mechanical degradation: membrane fracture caused by cycled constrains or fatigue imposed by varying temperature or humidity;
3. Shorting: an electronic current goes through the membrane because of an over-compression of the cell or topographical irregularities of the neighboring components leading to local over-compression and creep.

Almost the same point of view is taken here. First, chemical/electrochemical degradations, mechanical degradations and thermal ones are considered alternately. Then, two failures, shorting and gas crossovers, are reviewed.

Chemical/electrochemical degradation The chemical degradation is recognized as a major limiting process for the membrane lifetime [42]. It is attributed to actions of aggressive radical species that form during the functioning of the fuel cell and attack the vulnerable bonds of the polystyrene structure. PFSA membrane are widely used for their high chemical stability. However, perfluorinated materials are not inert during the stack functioning, above all when they are subject to voltage or humidity cycles.
This chemical degradation is characterized by the reducing thickness and the emission of HF, CO_2 et H_2SO_4 in output products of the stack. A reduced thickness leads to increased gas crossovers and mechanical weakness favorable for failures. The chemical degradation rate can be measured *in-situ* by quantifying the fluoride HF and monitoring the hydrogen crossover.
It is widely asserted that the attacks of aggressive and highly oxidant species cause the chemical degradation of PFSA membranes. Radicals sources and how they initiate their attacks are discussed in [17, 40, 42]. The functioning of PEMFCs at low relative humidities and high potentials often lead to high chemical degradation rates.
Finally, regarding chemical degradation, the contamination by foreign species can be mentioned. Corrosions of the stack components, impurities from gases or humidifier tanks can create a contamination with metallic impurities. Excess water can worsen this contamination by helping contaminants transport. The membrane is particularly vulnerable to foreign cations' presence because of their affinity of sulfonic acid groups. The cations take the protons places in the membrane and a loss of conductivity proportional to the cations ionic charge, and the consequent voltage loss, can be observed [40].

Mechanical degradation As it is partially constrained in the stack, the expansion and shrinkage of the

membrane with temperature or humidity changes can create mechanical constrains. Indeed, the operating conditions vary to follow the changing power demand and this can lead to hydrothermal fatigue. This fatigue may create mechanical degradation and failure by initiating and propagating microscopic cracks responsible of gas crossovers.
The constrained membrane is nominally maintained to a zero total strain that can compensate the hydrothermal strain to approximately 10% to 20%. Mechanical failures appear under different forms: cracks, tears, micro-holes or blisters. The lack of water also intervenes as a dry membrane is fragile and brittle. The penetration of particles from the catalyst may also create regions with high local constrains [40]. Current inversions also create damages as they imply local hot spot that can soften or even melt the membrane offering a new path for gas crossovers.
Under constant pressure, the PEM goes through a time-dependent deformation: creep. The creep of the polymer can cause a permanent thickness reduction and eventually failures (holes, etc.). Associated with chemical and other degradation, the impact become worse [17]. The creep of PFSA membranes has a low rate, this implies that catastrophic failures occurs after thousands of hours.

Thermal degradation The favorable temperature zone for the stack is located between 60 and 80°C. Membranes are subjected to critical ruptures at high temperature (80°C $\approx$ glass transition temperature) [19]. Proton conductivity decreases at high temperatures. It can be noticed that the Nafion structure is visibly affected for temperatures higher than 150°C, which is out the PEMFC temperature range.

Membrane shortings The ohmic shorting through the membrane is one of the main failure in the PEMFC. A shorting occurs when the electrons go directly from the anode to the cathode instead of through the device to power. Not only it reduces the performances of the stack, but it can also lead to heat generation and cause damages on the membrane.
Different challenges exist regarding the understanding of shortings evolution in the PEM [42] but the major difficulty is that shorting sites extremely local are hard to find. Researchers from General Motors distinguish two kinds of shorting [42]:

1. Soft shorts: little critical, they do not lead to immediate failure. Their exact cause is still under investigation, but it is widely asserted that the mechanical penetration into the membrane of external objects electronically conductive plays an important role.
2. Hard shorts: very critical, they result of thermal runaway from a soft short. They can lead directly to crossovers and failure of the cell. They can suddenly appear in a functioning stack in which a cell developed an ohmic resistance really higher than the others.

Gas crossover When the stack ages, hydrogen and oxygen can go through the membrane and to the opposite electrode. Oxygen crossover is not reported a lot in the literature. However, hydrogen crossover is well known to be a dramatic failure leading to the stack death. Indeed when a great quantity of hydrogen crosses and meets oxygen a combustion reaction occurs leading rapidly to the death of the stack.
Several studies such as [36, 43, 44] report that the crossover increases exponentially with time. A end of life threshold for the membrane subjected to hydrogen crossover is proposed in [15] corresponding to a crossover current of $10mA.cm^{-2}$.

Degradation modeling. A small review of constrain models for the membrane can be found in [42]. However, these models are behavioral models but they do not integrate the aging. An interesting model is proposed in [45]. The membrane is not modeled alone but with the electrodes to take into account more phenomena. All the chemical reactions contributing to degradation are modeled. The results show that the degradation progresses in a wavelike manner starting from the anode to the cathode. However, this modeling is to complex for prognostics and needs parameters that can hardly be reached in real world applications.

3.2.5. Sealing gaskets

Structure and role. The assembly of the membrane and electrodes includes sealing components to prevent hydrogen and air to mix but also to leak out of the stack. All the components should be perfectly aligned to maintain the appropriate closing pressure. This is important to reduce the contact resistances but also to avoid an over-compression of the GDLs. Sealing gaskets types can be divided into different categories that are reviewed in [46].

Degradation description. Sealing gasket degradation is still to be studied. Traces of decomposition products have been found in the membrane and the electrodes [19]. By degrading it looses its holding force: loss of compression, external leak of cooling or appearance of shorting. No degradation modeling can be found in the literature.

3.3. Component hierarchy

To create a hierarchy, some criteria have to be fixed. Here, instead of choosing one fix criterion, different questions are answered for all the components (Table 1). Then weights are given to the answers and a classification is deduced (Fig. 4). This classification might look subjective as it is based on the interpretation of the literature but it can be modified if some new elements appear in the analysis.

It appears that the membrane is the most critical component. It is not surprising as it is the only component which degradation can lead to the stack death because of too much gas crossovers. By looking at the components scores, it can be seen that components can be divided into different classes:

Table 1: Criteria for components classification

	Bipolar plates	GDL	Electrodes	Membrane	Sealing gaskets
Does the component has a role in producing the output energy?	Yes (+)	Yes (+)	Yes (+)	Yes (+)	No (-)
Does a failure leading to a loss of power exist? What is the importance of this power loss?	Yes (+) Weak (+)	Yes (+) Weak (+)	Yes (+) Strong (++)	Yes (+) Strong (++)	Yes[1] (+) Weak (+)
Does a failure preventing the components from filling partially or completely its functions exist?	No (-)	No (-)	No (-)	Yes (+)	Yes (+)
Does a failure leading to stack death[2] exist?	No (-)	No (-)	No (-)	Yes (+)	No (-)
Does the degradation vary with the current profile required?	Yes (+)	Yes (+)	Yes (+)	Yes (+)	Unknown
Total	2	2	3	7	1
Component ranking	3	4	2	1	5

[1] Even if the component does not participate to energy production, the corrosion products can create contaminations. [2] death refers to the impossibility for the stack to provide electricity

1. Class A: membrane and electrodes;
2. Class B: GDL and bipolar plates;
3. Class C: sealing gaskets.

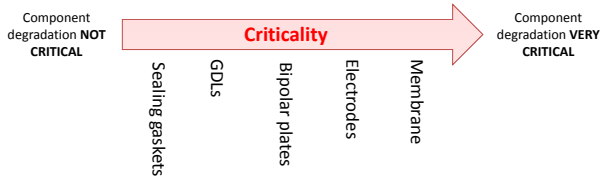

Figure 4: Proposed hierarchy of components invloved in the stack degradation

These classes allow distinguishing what are the components mandatory to include in the degradation model (class A), those which are optional (class B) and finally those which could be ignored (class C). Regarding this last comment, the study now focuses only on the electrodes and the membrane.

3.4. Degradation analysis

This section aims at analyzing more precisely the degradation mechanisms in both critical components.

3.4.1. Electrodes

Degradation classification. The degradation review shows that both electrodes do not degrade exactly the same way and that catalyst and carbon layers have to be considered separately. Before considering the electrodes separately, let's see how the degradation for both catalyst and carbon layers can be classified thanks to Tables 2 and 3. These tables are built to summarize but also to analyze the degradation reported in the previous section. They help separating the causes of the degradation and emphasizing its consequences. They are also used to assess the possibility of modeling and the necessity to take into account the different phenomena for prognostics.

Analysis and conclusions. The study of the degradation allowed separating the phenomena occurring at one electrode or at the other. Indeed, it was seen that the anode is almost unaffected by the loss of catalyst active area (Table 3). However, defining a clear hierarchy from these tables seems hard. Some new hypotheses have to be introduced.

First regarding the presence of impurities. They can come from the presence of CO or CO_2 due to carbon corrosion, of degradation products from the the bipolar plates, the membrane or the sealing gaskets, or from the presence of impurities in the reactants. Regarding these last ones, as the hydrogen used in lab experiments is very pure, this contamination can be neglected. But how can the contamination coming from the other components and from the corrosion be defined? The lack of knowledge and measurements impose to neglect these phenomena.

Then concerning the carbon support degradation, the question of gas starvation is raised. By hypothesis, enough reactant is continuously provided to the stack, but the degradation of transports in the GDL and the electrodes can lead to punctual events of local starvation. As they cannot be observed, these events are supposed scarce enough to be ignored. The hypothesis of continuous feeding, at stoichiometry above 1 and an open anode circuit, also allows stating that the corrosion at the anode can be neglected. Indeed, with the continuous flow, no lack of hydrogen should be observed, the small amount of water found at the anode is evacuated by the flow and the low potential at this electrode are elements that together allow neglecting the corrosion of the carbon support at the anode [47]. Still with carbon corrosion, it is clear that the current profile has to be included in the model, the basic events show that the current value might not be sufficient, the number of cycles as well as the time under OCV may appear too. It makes wondering if a precise modeling of carbon degradation is feasible and if the use of the carbon fingerprint proposed by [34] is adapted for a degradation model.

Table 2: Catalyst layer degradation

Components involved	Electrodes	
Degradation type	Electrochemical, chemical	
Causes	Contamination by impurities / carbon corrosion / crossovers Thickening due to particles movements + coalescence on carbon support Formation of metal oxides	
Consequences	On the component	Loss of active area / formation of Pt oxides Occupation of active sites by contaminants Sintering or migration of Pt on the carbon support Detachment and dissolution in the electrolyte
	On the functioning	Loss of activity
	On the other components	Formation of the Pt band in the membrane
Factors	Humidity/Acidic liquid environment, temperature Potentials between 0.85 and 1.4 V, OCV, cycles(current and temperature) Combination operating conditions / operating mode, presence of contaminants	
Time scales	Hours, days	
Criticality	Irreversible	
Degradation modeling available	Yes	
Importance for prognostics	Mandatory	
References	[6, 17, 18, 19, 31, 32, 34, 38, 37, 35, 36]	
Remarks	Loss of active area more important at the cathode than at the anode The anode is almost unaffected by Pt degradation whatever the conditions Catalyst charge would not have any influence on degradation Adsorption of some impurities can be reversible	

Regarding the loss of Pt active area, it comes from a complex interaction of different phenomena. To show that the fault tree of Fig. 5 is made. It shows the basic events of the loss of Pt active area and above all the strong interactions between them which form an inseparable block. Moreover the previous modeling analysis in section 3 proved that none of these events can be ignored to have a model close to reality. It imposes the use an empirical formulation with the loss of active area modeled by an exponential function. Nevertheless, this formulation is not so empirical as models like the one proposed by [6] demonstrated it.

3.4.2. Membrane

Degradation classification. The degradations and their consequent failures are numerous in the membrane, some may be eliminated before going further in the classification. The main causes of performance loss in the membrane are often classified as: mechanical degradation, thermal degradation, chemical degradation, shortings and contamination. In the study hypotheses (section 3.1.2), it is stipulated that the stack is functioning under nominal operating conditions. This hypothesis is extended and we suppose now the operating conditions allow always maintaining the inner temperature of the stack between 60 and 80°C. This enables saying that the thermal degradation of the membrane is not a primary cause of membrane failures. It may intervene, in particular with the creation of hot spots during shortings or H_2/O_2 reaction, but they are very fast phenomena and are taken into account with other events previously listed. The same kind of table than for the electrodes are proposed. They are separated in four: contamination (Table 4), mechanical degradation (Table 5), chemical degradation (Table 6) and shortings (Table 7). According to the causes and consequences highlighted in the tables, a new categorization of membrane's failures is proposed, Fig. 6.

Analysis and first conclusions. Among the main causes of the membrane's performance loss, the H_2 crossover is the only failure that can be measurable without taking the cell off the stack provided that there is no defect of impermeability. However, Its precise modeling may not be feasible but an approximation with the observed exponential tendencies can be a good solution.

Regarding the shorting, the soft are not detectable and the hard destroy rapidly the membrane (see section 3). Moreover, the lack of information on their origins and developing won't make any modeling possible. Consequently, they cannot be included directly in a prognostics model.

Then, the decrease in the proton conductivity appears because of a change in water repartition or because of a contamination. The change in water repartition can be due to different factors: aging of GDLs and electrodes, water accumulation, non uniform mass transport, etc. A precise modeling of temporal evolution of the membrane conductivity should contain a degradation part and behavioral part link to water production and repartition during operation.

Regarding contamination, the same problem than for the electrodes appears (i.e. not precise knowledge or measurement is available). So the same solution is adopted: the contamination is neglected. Finally, for the slowdown of the protons by the Pt band, the authors in

Table 3: Degradation of carbon support

Components involved	Electrodes	
Degradation type	Electrochemical, chemical	
Causes	Presence of water / properties of carbon used / current inversions Transition between cycles / reactant starvation / presence of gas crossover	
Consequences	On the component	Loss of active area / pores of the carbon surface become humid even hydrophilic
	On the functioning	Formation of CO / formation of CO_2
Observation	Direct measurements thanks CO and CO_2 produced	
Factors	Humidity, high temperatures, Potentials > 0.207 V, OCV / cycles of potentials	
Time scales	Hours, days	
Criticality	Irreversible	
Degradation modeling available	Yes	
Importance for prognostics	Mandatory	
References	[6, 17, 18, 19, 31, 32, 34, 38, 37, 35, 36]	
Remarks	CO production only occurs of the anode side	

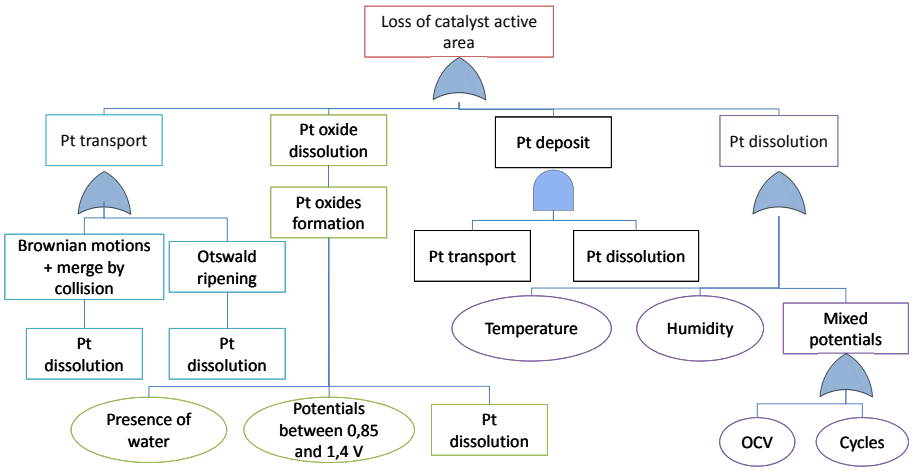

Figure 5: Loss of catalyst active area fault tree with the hypotheses set in section 3.1.2

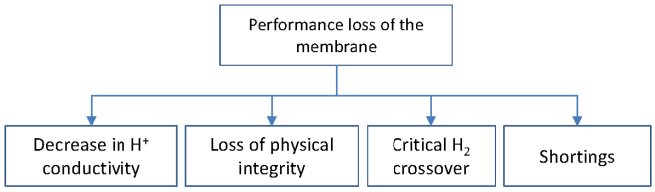

Figure 6: Main causes of performance loss of the membrane - new proposal

[49] assert that it is negligible, anyway its thickness and impact cannot be modeled.
By focusing on the last category of failure, namely the loss of physical integrity, the main thing to highlight is the interaction with all the other failures. Indeed, in addition to causing failures, it initiates some of the others. A modeling can be proposed but all the available mechanical models were only verified on pieces of membranes and out of the stack. Only the loss of thickness due to chemical degradation could be modeled but with parameters very hard to access.

This part allowed to set a classification of the components regarding the importance for prognostics. The membrane and the electrodes were retained as critical components and have to be modeled for prognostics. Some of the failure and degradation mechanisms to include in the degradation model have been selected, while other have been neglected due to the lack of knowledge or the limited data available. This can be used now to set the modeling for prognostics.

4. Semi empirical behavior model for prognostics

The previous analysis and review allow now building a degradation model that will be used for prognostics. But a new constrain appears: choosing the parameters to insert in the models. To guide this choice, the parameters that can be accessed on our lab test bench are reviewed.

Table 4: Contamination of the membrane

Component involved	Membrane	
Degradation type	Chemical	
Causes	Presence of cations / Pt migration / impurities in gases Products from corrosion of components	
Consequences	On the component	Replacement of protons by cations / Pt band
	On the functioning	Decrease in protonic conductivity / Performance's loss
Time scale	Hours, Days	
Criticality	Reversible and Irreversible	
Degradation modeling available	No	
Importance for prognostics	Mandatory	
References	[40]	

Table 5: Mechanical degradation of the membrane

Component involved	Membrane	
Degradation type	Mechanical	
Causes	Stresses linked to the assembly / local stress (ex: flow fields edge) Swelling and contraction with varying operating conditions Difference of expansion between reaction and non-reaction zones Loss of fluoride / loss of thickness by chemical degradation Penetrations of other components	
Consequences	On the component	Crack / tears / micro-holes, perforations Blisters / creep, deformations
	On the functioning	Increase in gas crossovers Initiation of destructive cycles (exothermic reactions)
Factors	Variations in relative humidity / increase in stresses / (increase in temperature)	
Time scale	Hours, days	
Criticality	Irreversible	
Degradation modeling available	Yes	
Importance for prognostics	Mandatory	
References	[17, 15, 36, 40, 42, 48, 45]	
Remarks	The creep of PFSA membrane is really slow, that's why catastrophic failures occur after thousands of hours.	

4.1. Physical parameters available

To create the model, we need to deal only with the parameters monitored continuously within the stack. For this study, as in most of applications, it is possible to access to: (1) stacks and individual cell voltages, (2) time, (3) reference and actual currents, (4) incoming and outgoing gases/water temperatures, (5) incoming and outgoing gases pressures, (6) relative humidities of incoming and outgoing gases and (7) stoichiometries. To complete the monitoring, punctual measurements of polarization curves and EIS are performed.
Even if some inaccessible parameters can be predicted thanks to prognostics, they should be in limited number to avoid injecting too much uncertainty in final prognostics estimates.

4.2. Modeling

4.2.1. Behavior modeling

Basic modeling. The starting point for the behavior modeling is the polarization curve equation. The model is first built at the cell level and then adapted to the stack level. Different formalizations for the polarization equation exist. The notations and formulation from [20] are used here as it distinguishes the contributions from both electrodes. The main idea is to start from the usual losses modeling, to select the parameters that age during a long term functioning and to replace them by a time-dependent expressions.
The polarization equation basically models the losses that impact the reversible cell voltage E_{rev}, also called the Nernst voltage. It is the voltage that would be obtained if all the Gibbs free energy was converted into electricity without any loss. The losses can be divided into four categories:

1. activation losses (E_{act});
2. concentration losses (E_{conc});
3. ohmic losses (E_{ohm});
4. and crossover losses (E_{cross});

The combination of these losses impacts the voltage, however each one has a different prevalence zone according to the current density, Fig. 7. Consequently, the polarization equation is given by:

Table 6: Chemical degradation of the membrane

Components involved	Membrane	
Degradation type	Chemical, Electrochemical	
Causes	Pt which migrated and deposit in the membrane Formation and attacks of radicals (amplified by crossovers) Presence of foreign cations	
Consequences	On the component	Loss of thickness / modification in material properties Mechanical fragility / loss of conductivity / initiation of perforations
	On the functioning	Emission of HF, CO_2, H_2SO_4 and others Increase in gas crossovers
Observation	Concentration of lost fluoride / measure of H_2 crossover	
Factors	Potential / OCV / humidity cycles / temperature variations	
Time scales	Hours, days	
Criticality	Irreversible	
Degradation modeling available	Yes	
Importance for prognostics	Mandatory	
References	[17, 40, 42]	

Table 7: Membrane shorting

Components involved	Membrane	
Degradation type	Electrochemical	
Causes	Penetration into the membrane of external objects electronically conductive, Increase in cell compression	
Consequences	On the component	Apparition of holes / Melting of the membrane
	On the functioning	Loss of performance / Generation of local heat
Observation	High deviation in ohmic resistance / potential abnormally high	
Time scale	Hours, days	
Criticality	Irreversible	
Degradation modeling available	No	
Importance for prognostics	To discuss	
References	[42]	
Remarks	No shorting development under 1 V	

$$E = E_{rev} - E_{conc+cross} - E_{ohm} - E_{act} \quad (2)$$

The impact of the concentration and crossover losses are gathered in a same term. This global model does not show the individual contributions of the electrodes and can be rewritten:

$$E = E_{rev} - E_{conc+cross,a} - E_{conc+cross,c} - E_{ohm} - E_{act,a} - E_{act,c} \quad (3)$$

where index a stands for anode and c for cathode.
As pure hydrogen diffuses better than oxygen in the nitrogen and water, the concentration losses at the anode can be neglected. The equation becomes:

$$E = E_{rev} - E_{act,a} - E_{act,c} - E_{conc+cross,c} - E_{ohm} \quad (4)$$

By replacing the losses by their expressions (please refer to [20] for more details), the polarization equation is now written as a function of i, the current density:

$$E(i) = E_{rev} - \frac{RT}{2\alpha_a F} ln(\frac{i_{loss} + i}{i_{0,a}}) - \frac{RT}{4\alpha_c F} ln(\frac{i_{loss} + i}{i_{0,c}}) - i(R_{ion} + R_{ele} + R_{cr}) + B_c ln(1 - \frac{i}{i_{max,c}}) \quad (5)$$

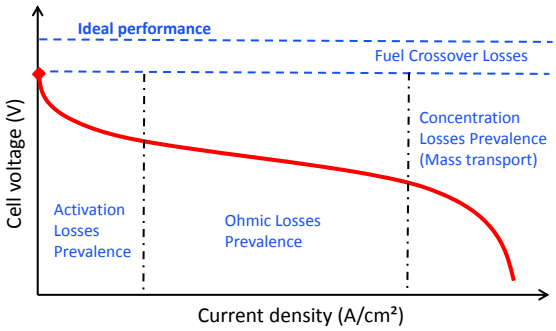

Figure 7: Representation of the different losses on the polarization curve

where:
- R is the gas constant equal to 8.3145 $J.mol^{-1}.K^{-1}$;
- T is the stack temperature kept constant;
- α_a and α_c are the charge transfer coefficients at the anode and at the cathode;
- F is the Faraday's constant equal to 96 485 $C.mol^{-1}$;
- i_{loss} represents the internal currents within the stack,

here we assume that it can be assimilated to the hydrogen crossover current alone and that no current caused by membrane shorting appears;
- $i_{0,a}$ and $i_{0,c}$ are the exchange current densities at each electrode;
- R_{ion}, R_{ele} and R_{cr} are respectively, the ionic, electronic and contact resistances;
- B_c is an empirical parameter allowing taking into account the effect of water and gas accumulations leading to non-uniform current densities on the electrode.
- $i_{max,c}$ is the limiting current at the cathode, it is the asymptotic value of the current for which the rate of disappearance of the product equals to the rate of their transport.

Introduction of the degradation. To select the parameters aging with time, the first step is to classify all the variables appearing in equation (5) into the three following categories:

1. *constants:* R, F;
2. *controlled:* T, P, E_{rev}, $i_{0,a}$, $i_{0,c}$, (the last three depend on T and P [20]) and i;
3. *aging:* α_a, α_c, i_{loss}, R_{ion}, R_{ele}, R_{cr}, B_c and $i_{max,c}$.

The parameters classified in the constant and controlled categories do not need to be justified but some of the other may need more explanations.
The charge transfer coefficients α_a and α_c depend on, at least, the material of the electrode, its microstructure and the reaction mechanisms (oxidation or reduction). The structure of the electrodes and its activity change with the aging. So it is logical to assume that the charge transfer coefficients vary. However, their values are very often set to make the polarization equation fit to the data, so it seems impossible with the current knowledge to guess how they vary with time.
Then based on the literature review and above all the conclusions of its analysis, modelings for the parameters' degradation can be proposed. First, regarding i_{loss}, as we assimilate it to the hydrogen crossover current, the modeling that seems the best suitable here is the exponential modeling (section 3.4.2):

$$i_{loss}(t) = i_{loss,0} exp(b_{loss} t) \tag{6}$$

Indeed, this trend is shown in the great majority of the experiments reported in the literature and other models have not been fully validated until now (section 3.2.4).
Next parameters are the resistances appearing in the ohmic loss term. In the initial formulation, three resistances are distinguished: ionic, electronic and contact resistances. As electronic and contact resistance can be difficult to study separately, they are gathered in a same variable $R = R_{ele} + R_{cr}$. From the measurements reported in different studies, its aging can be defined by:

$$R(t) = R_0 + b_R t \tag{7}$$

Regarding the ionic resistance linked to the membrane, recent results published in [50] show that the conductivity as well as the water uptake and the ion exchange capacity for the pieces of membrane in different Nafion decrease exponentially as function of time. This is confirmed by some studies showing an exponential increase in the resistance [43]:

$$R_{ion}(t) = R_{ion,0} exp(b_{ion} t) \tag{8}$$

Although this expression assume that only time influences the conductivity and not contamination or water repartition changes, this hypothesis will be kept afterward.
Finally, the two variables of the activation losses have to be considered. As stated before, B_c allows taking into account the effect of water and gas accumulations leading to non-uniform current densities on the electrode. Both degradation and operating events may affect these accumulations and so make B_c value change. The degradation of the GDL, mainly the loss of hydrophobicity, strongly impacts the diffusion but also the content of water and its distribution and accumulation in the electrode compartment. This should impact B_c by an increasing in this value during aging. However, the water and gas distribution are also affected by reversible phenomena (Section 2.2.1) and this also influences B_c but it is hard to say in which proportion. The following modeling is proposed:

$$B_c(t) = B_{c,0} + b_B t \tag{9}$$

The same idea has to be employed to model $i_{max,c}$. Indeed, according to [28], the limiting current density of the cathode can be written: $i_{c,L} = \frac{4F}{RT}\left(\frac{D_{O_2}}{L_{GDL}}\right) P_{O_2}$, where D_{O_2} is the diffusivity of oxygen, P_{O_2} the pressure of the oxygen at the cathode and L_{GDL} the thickness of the GDL. In this expression, the thickness of the GDL may be affected by the carbon corrosion during the aging and the diffusivity may be influenced by degradation and reversibilities in the same way that of B_c. As the thickness of the GDL may not vary from more than some μm, the choice not to model its decrease during aging is made. For the diffusivity, the same modeling as for B_c is used:

$$D_{O_2}(t) = D_{O_2,j} + b_D t \tag{10}$$

Equations (9) and (10) are hard to justify physically. The linear expressions are inspired by the results we had in [7]. Indeed, the aging parts (see Fig. 2) show among others a linear component (combined with other mathematical functions) that may include the effect of water and gas accumulation that influence the diffusivity.

One last thing to do is to replace the current density value by a function of the current imposed to the stack I:

$$i(t) = \frac{I(t)}{A(t)} \tag{11}$$

where $A(t)$ is the active area of the electrode that decrease with the aging given by an exponential form. By extracting some aging data of this area from graphs proposed in the literature, it can seen that a simple exponential does not describe properly the aging (Fig. 8). Consequently, the expression used is:

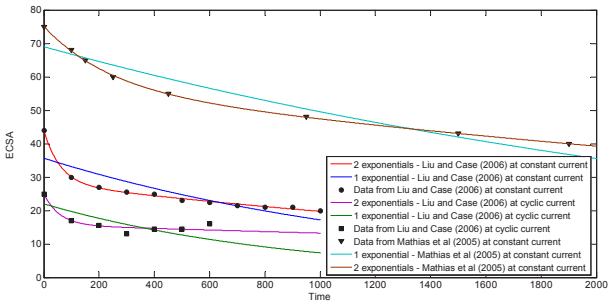

Figure 8: Exponential modeling of the aging of the active area with example taken from [37, 36]

$$A(t) = A_0 exp(b_{A1}t) + A_1 exp(b_{A2}t) \quad (12)$$

with A_0 equals to the theoretical geometric size of the active area and A_1 is contained in $[-1\%, 1\%]$ and reflects the error that can exist on the actual size of the active area. Physically, it cannot be justified. However, the model proposed by [49] seems to go in the same way.
The model described by equation (5) is built for a single cell. It is multiplied by the number of cells (n) to obtain the stack voltage. However, some works tend to show that all cells do not degrade in the same way within the stack [51, 52]. The cells next to the edges of the stack degrade faster and this impacts the global voltage. Consequently, the classical expression $V_{stack} = n.V_{cell}$ has to be modified to include this heterogeneity. For that purpose, a corrective term written p is introduced as no existing study allows to quantify the degradation differences within a stack. The equation of power becomes: $P_{stack} = n.P_{cell} - p$. The final expression of the power delivered by the stack is:

$$\begin{aligned} P(I,t) = nI(t)[&E_{rev} \\ &- \frac{RT}{2\alpha_a F} ln\left(\frac{i_{loss,0}e^{b_{loss}t} + \frac{I(t)}{A_0 e^{b_{A1}t} + A_1 e^{b_{A2}t}}}{i_{0,a}}\right) \\ &- \frac{RT}{4\alpha_c F} ln\left(\frac{i_{loss,0}e^{b_{loss}t} + \frac{I(t)}{A_0 e^{b_{A1}t} + A_1 e^{b_{A2}t}}}{i_{0,c}}\right) \\ &- \frac{I(t)}{A_0 e^{b_{A1}t} + A_1 e^{b_{A2}t}}(R_{ion,0}e^{b_{ion}t} + R_0 + b_R t) \\ &+ (B_{c,j} + b_B t) ln\left(1 - \frac{\frac{I(t)}{A_0 e^{b_{A1}t} + A_1 e^{b_{A2}t}}}{\frac{4F}{RT}\left(\frac{D_{O_2,j} + b_D t}{L_{GDL}}\right) P_{O_2}}\right)] - p \end{aligned} \quad (13)$$

It is important to mention that the dependency of the degradations to the current magnitude is not explicitly written in the model. In practice, it implies that the coefficients of the model driving the evolution of some degradations such as b_{loss}, b_R, etc. can evolve with time.

5. Behavioral model validation

A validation of the models is performed in this section, it comes in two steps. The first step proves that the model can be identified and matches to the datasets available with their different characteristics. Then, a sensitivity analysis is proposed to reinforce the validation.
To assess the generic nature of the model, different cases of mission profiles are considered: constant current, current ripples and μ-CHP profile. By proceeding gradually with the magnitude of the current variations, it allows evaluating the advantages and the limits of the model in different cases.

5.1. Description of the data

Raw data are represented by the blue curves in Fig. 13 to Fig. 15.

5.1.1. Constant current profile

Two datasets are available for this case. The first one is referred as D1. It comes from a PEMFC stack containing five cells with an active area of $100cm^2$ aged during 1750 hours at a constant current of 60 A. The second one, D2, also comes from a 5-cell stacks with active areas of $100cm^2$ but aged only during 985 hours at a constant current of 70 A. More details on D2 are available in [53]. Both datasets are measured from stacks of the same manufacturer, UBzM. For both datasets, polarization curves measured along the aging are available.

5.1.2. Current ripples

The idea of the current ripple profile is to emulate the behavior of a static converter connected to the stack output. This stack, as D1 and D2, is also provided by UBzM and has an active area of 100 cm^2. It aged during a bit more than 1000 hours. The nominal current used is 70 A and small triangle ripples of $\pm 10\%$ at 1kHz [53]. This dataset is now referred as D3.

5.1.3. Micro-CHP mission profile

The fourth dataset, named D4, comes from a different stack technology (Technology G from CEA LITEN). The stack is composed of 8 cells with a total active area of 220 cm^2. The mission profile used for the experiments is punctuated by characterizations and is proposed on Fig. 9.

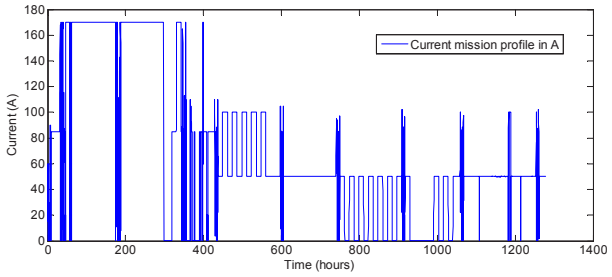

Figure 9: Mission profile applied to the 8-cell stack D4

5.2. Data processing

Raw power data contain a lot of information and the degradation is drowned among them. The model previously described focuses only on degradations which are phenomena with time constants equal or greater than the hour whereas the data are recorded with a frequency of 1Hz. So the data have to be filtered.

Filtering could be performed at different levels of fuel cell data: (1) noise filtering, (2) reduction of fast phenomena dynamics, (3) outliers filtering and (4) reduction of transients. A frequency analysis of the power signals (not detailed here) shows that elements (1) and (2) can be reduced with a low-pass filter. A simple technique, almost without dephasing if the lag is well-chosen, is the moving average (MA). Basically, a choice is made between different variants: simple MA, exponential MA, weighted MA, etc. Some tests show that the simple MA algorithm with a window of 20 hours is sufficient to eliminate noise and fast dynamics.

Due to the low speed of degradations, keeping one point per hour is enough whereas the data acquisition frequency is 1Hz. As the degradation indicators do not evolve significantly in an hour, a simple data reduction is to keep the point recorded at the beginning of each hour. The data filtered and reduced are drawn in yellow in Fig. 13 to Fig. 15.

Finally, reversible phenomena have to be removed. It is interesting to notice that not all datasets need to be smoothed. Indeed, D4 (μ-CHP profile) looks almost unaffected by recoveries or transient regimes. A possible explanation is the following. When the current level is modified to follow the mission profile, stoechioemetries are maintained constant to keep the stack in its nominal conditions. This implies that the gas flows are modified and may help homogenizing gas and liquid distribution within the stack. If that hypothesis is true, it means that the power measured with profile using variable currents shows almost only the degradation. Consequently, it does not need any smoothing.

The robust loess algorithm is used to smooth the data. To find a good trade-off between keeping to much information about the reversible phenomena and loosing degradation information during the smoothing, a simple procedure is designed. First, the derivative of the smoothed signal is calculated. As the degradations create a continuous power loss, the derivative of the smoothed signal should be almost constant and equal to 0. Then, based on the different datasets, it is assumed that the stack spends almost 25% of its lifetime in transient regimes (including characterizations). So, it can be deduced that the signal is well-smoothed when its derivative has 75% of its components equal to 0. The smoothed signals are the green curves in Fig. 13 and in Fig. 14.

5.2.1. Initial polarization curve estimate

To start the model identification, the initial polarization curve made before the aging is estimated. Some unknown parameters called Set 1 (see Table 8) are initialized. All parameters are estimated using a least square algorithm thanks the fitting toolbox of Matlab software.

Table 8: Sets of parameters

Set 1	α_a, α_c, $i_{0,a}$, $i_{0,c}$, $i_{loss,0}$, A_1, $R_{ion,0}$, R_0, $B_{c,0}$, $D_{O_2,0}$
Set 2	b_{loss}, b_{A1}, b_{A2}, b_{ion}, b_R, b_B, b_D, p

To initialize the test procedure, distributions of possible values for the parameters are built thanks to the literature and adjusted according to the data. Indeed, to obtain a convincing fitting, all the values should reflect the reality and respect some constrains (note that in some cases these values could be accessed with measurements if the proper equipment is available). As an example, α_a and α_c should be in the interval $[0, 1]$ and their sum equal or close to 1. The intervals proposed for the fitting initialization are available in Table 9. They are built thanks to expert knowledge and literature.

Table 9: Estimate values of parameters

α_a	[0.5 0.8]	b_{loss}	[0.001 0.009]
α_c	[0.1 0.5]	A_1	[-1 1]
$i_{loss,0}$	[0.001 0.1]	b_{A1}	[0 Inf]
$i_{0,a}$	[0 0.01]	b_{A2}	[-1 1]
$i_{0,c}$	[0 0.01]	b_{ion}	[0 0.001]
$R_{ion,0}$	[0 0.09]	b_R	[0 0.001]
R_0	[0 0.09]	$b_{B,aging}$	[0 0.1]
$B_{c,0}$	[0 5]	$b_{D,aging}$	[0.0001 0.01]
$D_{O_2,0}$	[0.1 0.9]	p	[-5 0]

The first polarization curve is estimated at t=0 hours. This eliminates time-depending terms in equation (13) allowing the initialization of the Set 1. The curve estimation as well as the error coming with he estimates are shown on Fig. 10 for both datasets.

It can be seen on Fig. 11 that the estimation error remains mostly lower than 0.05 V (i.e. between 1% and 1.5% depending of the current) for both datasets and raises to 0.15V (i.e. 5%) for extreme currents. Also, it seems that the concentration losses part creates the greatest error for both cases. Two reasons can be assumed: the coefficients leading that part of the model are not well-estimated or the anode concentration losses should have not been neglected. To eliminate the second possibility, a fitting including the anode concentration losses as in equation (3) is performed.

The results between polarization curves based on equations (3) and (4) are compared on Fig. 12. The residuals are globally of the same magnitude of order. The red curve with stars representing Equation (3) shows that even if the high current part is slightly better approximated, the error in the low current part increases. It can be concluded from that comparison that ignoring the anode concentrations losses does not impact strongly the results and this assumption can be kept to pursue that work.

Once this polarization curve obtained, the power can be

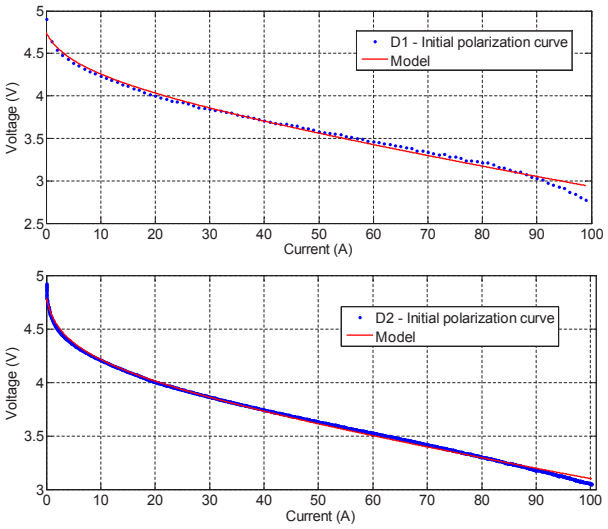

Figure 10: Initial polarization curves for D1 and D2

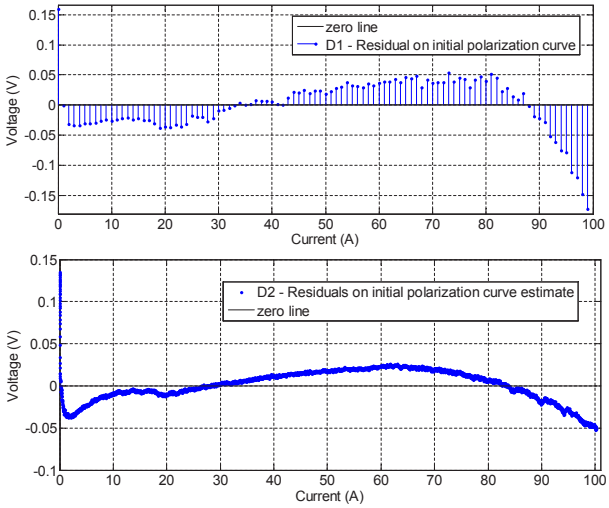

Figure 11: Residuals on initial polarization curve estimates for D1 and D2

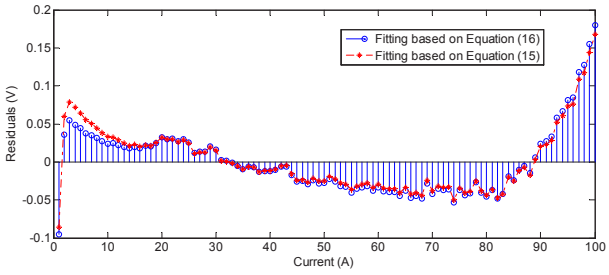

Figure 12: Residuals on polarization curve estimates with and without inclusion of anode concentration losses, equations (3) and (4)

estimated.

5.2.2. Power behavior estimate

Set 2 is identified by fitting equation (13) to the power data, again with a least square algorithm. Both time and current are now varying.

The final results for D1 and D2 are presented in red in Fig. 13, while they appear in Fig. 14 and Fig. 15 for D3 and D4. By comparing the model and the data, it can be seen that the global aging trend is well-followed by the model for all datasets.

To help evaluating the model, the coefficient of determination R2 according to the raw data are calculated. For D1, R2 = 0.9890 is obtained; for D2, R2 = 0.9616; for D3, R2 = 0.9822 and for D4, R2 = 0.9958. All are higher than 0.9, it validates the model for the three types of mission profiles.

5.3. Sensitivity analysis

To further validate the model and also to help using it more easily, a sensitivity analysis (SA) is performed. SA allow determining if the model reflects the reality by checking that among the most influent variables, none of them was initially supposed to play a minor role. SA also help choosing which variables can be fixed without creating a major error on the model output [54]. There are two classes of SA [55, 56]:

1. screening methods for models with a great number of variables (>10);
2. quantitative methods that can be distinguished into local and global SA preferred for models with a low number of variables.

In this study, quantitative methods are considered. Local sensitivity can be defined as the sensitivity at a fixed point in the parameter space, while global sensitivity is the integrated sensitivity over the entire input space [55]. Based on these definitions, a global SA is preferred. Indeed, it shows how the variability of the inputs affects the variability of the output.

To perform the SA, the Matlab toolbox called GSAT and proposed by the author of [55] is used. It gives the sensitivity of the model to its parameters based on Sobol' indexes. There are different order for the Sobol' indexes, but a first order index is sufficient for this SA. It gives the sensitivity of the output to one parameter and is expressed as:

$$Si = \frac{V(E[Y|Xi])}{V(Y)} \tag{14}$$

where Y is the model output, Xi one of the input parameters, $V()$ is the variance and $E[]$ the expectation. Si is a value between 0 and 1:

- if $0.8 < Si < 1$, the sensitivity to Xi is very important;
- if $0.5 < Si < 0.8$, the sensitivity to Xi is important;
- if $0.3 < Si < 0.5$, the sensitivity to Xi is unimportant;

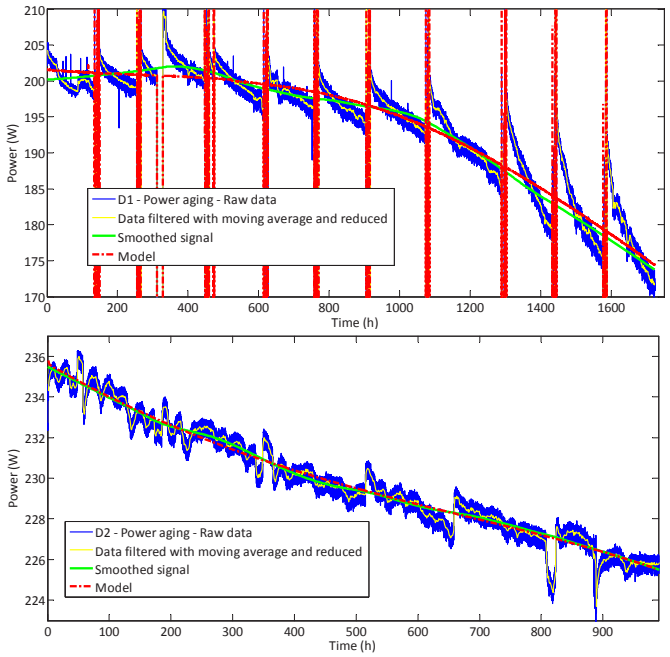

Figure 13: Upper part: Power supplied by the 5-cell stack D1 measured experimentally versus aging time at 0.6 A/cm2 and comparison with the model. Lower part: Power supplied by the 5-cell stack D2 measured experimentally versus aging time at 0.7 A/cm2 and comparison with the model

- if $0 < Si < 0.3$, the sensitivity to Xi is irrelevant;

The sum of all the Si is equal to 1.
To limit the number of input variables, it is decided to perform the SA once the set of parameters called Set 1 is identified. It makes sense as the parameters come from a classic identification the polarization curve at $t = 0$ and it is well-known that, except the current, only the parameters guiding the linear part of the model, i.e. the resistances, have the greatest importance.
Consequently, the SA is limited to the 8 parameters of Set 2, to which are added the current and time. The possible values for each input are proposed in Table 9, I that can

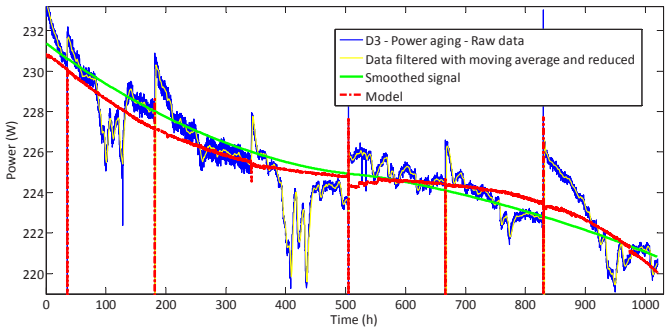

Figure 14: Power supplied by the 5-cell stack D3 measured experimentally versus aging time with ripples of 1Hz around 0.7 A/cm2 and comparison with the model

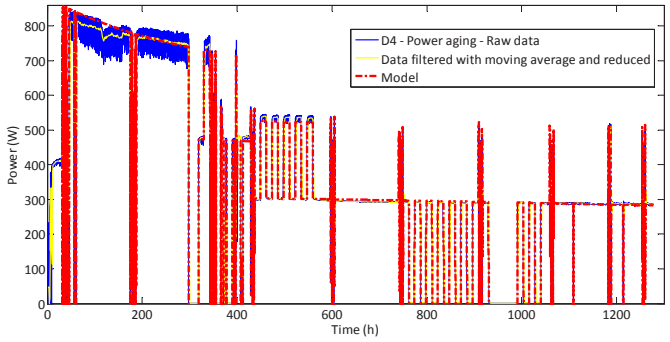

Figure 15: Power supplied by the 8-cell stack D4 measured experimentally versus aging time with a varying mission profile and comparison with the model

vary from 0 to 180A and t from 1 to 3000 hours. The SA's results are presented in Table 10.

Table 10: Sobol' indexes of the model inputs

Input	I	t	b_{loss}	b_{A1}	b_{A2}	b_{ion}
Si	0,64	0,15	0,09	2,6e-05	1,6e-06	3,8e-07

b_R	$b_{B,aging}$	$b_{D,aging}$	p
5,2e-06	1,8e-06	6,1e-06	4,7e-05

As expected, the current is the most important input, followed by the time. It is coherent with the goal of the model which is to follow the power evolution according to the mission profile during time. All the other parameters have negligible impacts on the output.
It is also interesting to go further and wonder what happens if there is a constant current profile. Indeed, in that case only the degradations are supposed to influence the power. And it is important to identify which part of the model mostly drives the power loss at a constant current. In that case St goes up to 0.54 and Sb_{loss} to 0.35. The conclusion is unsurprising, time affects the power loss. It also seems that the hydrogen crossover is the most critical part of the model and it is coherent with the conclusion of the previous degradation analysis.
These sensitivity analyses show that the model reflects well the reality and confirm the results obtained by fitting the model to the data. It will also greatly help to use the model in the context of prognostics. Indeed, it is now known that a great majority of parameters that were supposed to evolve with time could be fixed.

5.4. Discussion

The first point to discuss is the parameter identified values. As the initialization intervals were all built to give plausible results, the coherence with the order of magnitude of real measurements is considered as correct.
A question harder to discuss is: can these values be the real values ? For α_a and α_c, the sum for all datasets is

close to 1 so they can be realistic values. However, for the great majority of all the resting parameters in Set 1 such as $i_{loss,0}$, $R_{ion,0}$, R_0 or $D_{O_2,0}$ with no measurements on the cells prior to the aging, no answer can be given, same for Set 2. A possible argument that would make the answer tend to a no, is that the computing of the least square can give good fitting with completely different initializations.

5.5. Going further towards model validation

The model validation is already satisfying but far from complete. Indeed, the datasets tested in this paper are quite short and do not exhibit dramatic degradations. Moreover, the lack of data did not enable performing health assessment on an automotive profile. A first step toward a validation on automotive profiles can be made thanks to a short dataset of only 42 hours obtained from a similar stack as D4. The mission profile alternate a current I1 = 5A during 10 seconds with I2 = 100A during 50s. The length of the data does not allow speaking about validation. However, it can help observing if the model is able to follow mission profiles with fast current variations. The estimated power is obtained with R2 = 0.99 on the 42 hours. It is encouraging to see that a model designed for a time scale in hours can be adapted to a mission profile varying in seconds.

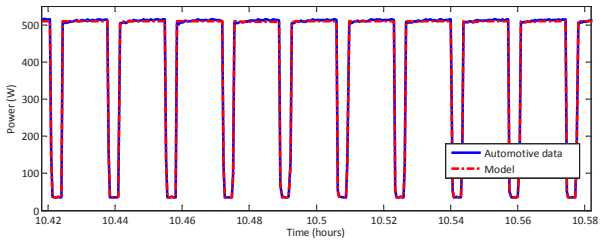

Figure 16: Power estimations for the 8-cell stack aged with an automotive profile

Another part of the validation process is the use of the model for prognostics. Successful attempts are proposed in [57, 58] but are not yet perfect and need to be reinforced.

6. Conclusion

This paper proposes a complete analysis to perform prognostics of PEMFC. A framework is presented to help applying PHM to a PEMFC stack, by mapping all the factors influencing the two most important outputs of such a system: the power it delivers and its lifetime. To complete the framework, a proper vocabulary definition is proposed. Once the limits of the study fixed, a deep literature review on the stack degradation, integrating some of the most recent understanding of the phenomena serves as a basis for a complete degradation and failure analysis. This analysis shows that, unsurprisingly, the electrodes and the membrane are the most critical components of the stack when degradation is concerned. For both of them, a certain number of degradations are selected and modeled. It allows building a degradation model capable of following the aging of the power accurately. Indeed, the model shows coefficients of correlation higher than 0.96 for four different datasets obtained with both constant and varying mission profiles. This enables validating this new model for health assessment of a PEMFC stack.
Next steps of this work consist in, first, testing the model on longer variable mission profiles such as automotive ones. And then, the model has to be integrated in a prognostics framework to obtain accurate RUL predictions.

7. Acknowledgement

The authors would like to thank the ANR project PROPICE (ANR-12-PRGE-0001) and the Labex ACTION project (contract "ANR-11-LABX-01-01") both funded by the French National Research Agency for their support.

References

[1] M. Jouin, R. Gouriveau, D. Hissel, M.-C. Péra, N. Zerhouni, Prognostics and health management of PEMFC state of the art and remaining challenges, Int. J. of Hydrogen Energy 38 (35) (2013) 15307 – 15317.
[2] R. Gouriveau, N. Zerhouni, Connexionist-systems-based long term prediction approaches for prognostics, IEEE Tr. on Reliability 61 (4) (2012) 909–920.
[3] R. Silva, R. Gouriveau, S. Jemei, D. Hissel, L. Boulon, K. Agbossou, N. Y. Steiner, Proton exchange membrane fuel cell degradation prediction based on adaptive neuro fuzzy inference systems, Int. J. of Hydrogen Energy 39 (21) (2014) 11128 – 11144.
[4] A. Hochstein, H.-I. Ahn, Y. T. Leung, M. Denesuk, Switching vector autoregressive models with higher-order regime dynamics, in: IEEE PHM conference 2014, 2014, pp. 1–10.
[5] T. Kim, H. Kim, J. Ha, K. Kim, J. Youn, J. Jung, B. D. Youn, A degenerated equivalent circuit model and hybrid prediction for state-of-health (SOH) of PEM fuel cell, in: IEEE PHM conference 2014, 2014, pp. 1–7.
[6] X. Zhang, P. Pisu, An unscented kalman filter based approach for the health-monitoring and prognostics of a polymer electrolyte membrane fuel cell, in: Proc. of the annual conference of the prognostics and health management soc., 2012.
[7] M. Jouin, R. Gouriveau, D. Hissel, M.-C. Péra, N. Zerhouni, Joint particle filters prognostics for PEMFC power prediction at constant current solicitation, IEEE Tr. on Reliability-doi:10.1109/TR.2015.2454499.
[8] M. Bressel, M. Hilairet, D. Hissel, B. Ould Bouamama, Dynamical modeling of proton exchange membrane fuel cell and parameters identification, in: 6th International Conference Fundamentals and Development of Fuel Cells, FDFC'15., Toulouse - France, 2015.
[9] P. Khayyer, A. Izadian, P. Famouri, Reliability investigation of a hybrid fuel cell electric vehicle powered by downsized fuel cells, in: Technological Developments in Education and Automation, Springer Netherlands, 2010, pp. 495–497.
[10] M. Gerbec, V. Jovan, J. Petrovcic, Operational and safety analyses of a commercial PEMFC system, Int. J. of Hydrogen Energy 33 (15) (2008) 4147 – 4160.
[11] L. Placca, R. Kouta, Fault tree analysis for PEM fuel cell degradation process modelling, Int. J. of Hydrogen Energy 36 (19) (2011) 12393 – 12405.

[12] M. Whiteley, S. J. Dunnett, L. Bartlett-Jackson, Fault tree analysis of polymer electrolyte fuel cells to predict degradation phenomenon, in: Advances in Risk and Reliability Technology Symposium 2013, Loughborough University, 2013.
[13] N. Yousfi Steiner, D. Hissel, P. Moçotéguy, D. Candusso, D. Marra, C. Pianese, M. Sorrentino, Application of fault tree analysis to fuel cell diagnosis, Fuel Cells 12 (2) (2012) 302–309.
[14] C. Wieland, O. Schmid, M. Meiler, A. Wachtel, D. Linsler, Reliability computing of polymer-electrolyte-membrane fuel cell stacks through petri nets, J. of Power Sources 190 (1) (2009) 34 – 39.
[15] F. De Bruijn, V. Dam, G. Janssen, Review: durability and degradation issues of pem fuel cell components, Fuel Cells 8 (1) (2008) 3–22.
[16] S. Kundu, M. Fowler, L. Simon, S. Grot, Morphological features (defects) in fuel cell membrane electrode assemblies, J. of Power Sources 157 (2) (2006) 650 – 656.
[17] R. Borup, J. Meyers, B. Pivovar, Y. S. Kim, R. Mukundan, D. Garland, N.and Myers, F. Wilson, M.and Garzon, D. Wood, et al., Scientific aspects of polymer electrolyte fuel cell durability and degradation, Chemical reviews 107 (10) (2007) 3904–3951.
[18] W. Schmittinger, A. Vahidi, A review of the main parameters influencing long-term performance and durability of PEM fuel cells, J. of Power Sources 180 (1) (2008) 1 – 14.
[19] J. Wu, X. Z. Yuan, J. J. Martin, H. Wang, J. Zhang, J. Shen, S. Wu, W. Merida, A review of PEM fuel cell durability: Degradation mechanisms and mitigation strategies, J. of Power Sources 184 (1) (2008) 104 – 119.
[20] O. Z. Sharaf, M. F. Orhan, An overview of fuel cell technology: Fundamentals and applications, Renewable and Sustainable Energy Reviews 32 (2014) 810 – 853.
[21] U. Lucia, Overview on fuel cells, Renewable and Sustainable Energy Reviews 30 (0) (2014) 164 – 169.
[22] European Standard EN 13306, British Standards Institution, 2001.
[23] M. Prasanna, E. Cho, T.-H. Lim, I.-H. Oh, Effects of MEA fabrication method on durability of polymer electrolyte membrane fuel cells, Electrochimica Acta 53 (16) (2008) 5434 – 5441.
[24] S. Kundu, M. Fowler, L. C. Simon, R. Abouatallah, Reversible and irreversible degradation in fuel cells during open circuit voltage durability testing, J. of Power Sources 182 (1) (2008) 254 – 258.
[25] U. S. Department of Energy, The department of energy hydrogen and fuel cells program plan (2011).
URL http://www.hydrogen.energy.gov/roadmaps_vision.html
[26] M. Knowles, D. Baglee, A. Morris, Q. Ren, The state of the art in fuel cell condition monitoring and maintenance, World Electric Vehicle Journal 4.
URL http://sure.sunderland.ac.uk/3795/
[27] H. Tawfik, Y. Hung, D. Mahajan, Chapter 5 - bipolar plate durability and challenges, in: M. M. Mench, E. C. Kumbur, T. N. Veziroglu (Eds.), Polymer Electrolyte Fuel Cell Degradation, Academic Press, 2012, pp. 249 – 291.
[28] J. M. Morgan, R. Datta, Understanding the gas diffusion layer in proton exchange membrane fuel cells, J. of Power Sources 251 (2014) 269 – 278.
[29] G. Chen, H. Zhang, H. Ma, H. Zhong, Electrochemical durability of gas diffusion layer under simulated proton exchange membrane fuel cell conditions, Int. J. of Hydrogen Energy 34 (19) (2009) 8185 – 8192.
[30] J. Pauchet, M. Prat, P. Schott, S. P. Kuttanikkad, Performance loss of proton exchange membrane fuel cell due to hydrophobicity loss in gas diffusion layer: Analysis by multiscale approach combining pore network and performance modelling, Int. J. of Hydrogen Energy 37 (2) (2012) 1628 – 1641.
[31] S. S. Kocha, Chapter 3 - electrochemical degradation: Electrocatalyst and support durability, in: M. M. Mench, E. C. Kumbur, T. N. Veziroglu (Eds.), Polymer Electrolyte Fuel Cell Degradation, Academic Press, 2012, pp. 89 – 214.
[32] P. Parthasarathy, A. V. Virkar, Electrochemical ostwald ripening of pt and ag catalysts supported on carbon, J. of Power Sources 234 (2013) 82 – 90.
[33] J. Durst, A. Lamibrac, F. Charlot, J. Dillet, L. F. Castanheira, G. Maranzana, L. Dubau, F. Maillard, M. Chatenet, O. Lottin, Degradation heterogeneities induced by repetitive start/stop events in proton exchange membrane fuel cell, Applied Catalysis B: Environmental 138-139 (2013) 416–426.
[34] S. Dhanushkodi, M. Tam, S. Kundu, M. Fowler, M. Pritzker, Carbon corrosion fingerprint development and de-convolution of performance loss according to degradation mechanism in PEM fuel cells, J. of Power Sources 240 (2013) 114 – 121.
[35] R. M. Darling, J. P. Meyers, Kinetic model of platinum dissolution in pemfcs, J. of The Electrochemical Soc. 150 (11) (2003) A1523–A1527.
[36] D. Liu, S. Case, Durability study of proton exchange membrane fuel cells under dynamic testing conditions with cyclic current profile, J. of Power Sources 162 (1) (2006) 521 – 531.
[37] M. F. Mathias, R. Makharia, H. A. Gasteiger, J. J. Conley, T. J. Fuller, C. J. Gittleman, S. S. Kocha, D. P. Miller, C. K. Mittelsteadt, T. Xie, et al., Two fuel cell cars in every garage?, Electrochemical Soc. 14 (3) (2005) 24–36.
[38] W. Bi, T. F. Fuller, Modeling of PEM fuel cell pt/c catalyst degradation, J. of Power Sources 178 (1) (2008) 188 – 196.
[39] W. Bi, Q. Sun, Y. Deng, T. F. Fuller, The effect of humidity and oxygen partial pressure on degradation of pt/c catalyst in PEM fuel cell, Electrochimica Acta 54 (6) (2009) 1826 – 1833.
[40] A. Collier, H. Wang, X. Z. Yuan, J. Zhang, D. P. Wilkinson, Degradation of polymer electrolyte membranes, Int. J. of Hydrogen Energy 31 (13) (2006) 1838 – 1854.
[41] S. Peighambardoust, S. Rowshanzamir, M. Amjadi, Review of the proton exchange membranes for fuel cell applications, Int. J. of Hydrogen Energy 35 (17) (2010) 9349 – 9384.
[42] C. S. Gittleman, F. D. Coms, Y.-H. Lai, Chapter 2 - membrane durability: Physical and chemical degradation, in: M. M. Mench, E. C. Kumbur, T. N. Veziroglu (Eds.), Polymer Electrolyte Fuel Cell Degradation, Academic Press, 2012, pp. 15 – 88.
[43] T.-C. Jao, G.-B. Jung, S.-C. Kuo, W.-J. Tzeng, A. Su, Degradation mechanism study of ptfe/nafion membrane in MEA utilizing an accelerated degradation technique, Int. J. of Hydrogen Energy 37 (18) (2012) 13623 – 13630.
[44] B. Wu, M. Zhao, W. Shi, W. Liu, J. Liu, D. Xing, Y. Yao, Z. Hou, P. Ming, J. Gu, Z. Zou, The degradation study of nafion/ptfe composite membrane in PEM fuel cell under accelerated stress tests, Int. J. of Hydrogen Energy 39 (26) (2014) 14381 – 14390.
[45] A. Shah, T. Ralph, F. Walsh, Modeling and simulation of the degradation of perfluorinated ion-exchange membranes in pem fuel cells, J. of The Electrochemical Soc. 156 (4) (2009) B465–B484.
[46] D. hao Ye, Z. gang Zhan, A review on the sealing structures of membrane electrode assembly of proton exchange membrane fuel cells, J. of Power Sources 231 (2013) 285 – 292.
[47] A. Pandy, Z. Yang, M. Gummalla, V. V. Atrazhev, N. Y. Kuzminyh, V. I. Sultanov, S. Burlatsky, A carbon corrosion model to evaluate the effect of steady state and transient operation of a polymer electrolyte membrane fuel cell, J. of The Electrochemical Soc. 160 (9) (2013) F972–F979.
[48] K. D. Baik, B. K. Hong, M. S. Kim, Effects of operating parameters on hydrogen crossover rate through nafion membranes in polymer electrolyte membrane fuel cells, Renewable Energy 57 (2013) 234 – 239.
[49] X. Zhang, P. Pisu, Prognostic-oriented fuel cell catalyst aging modeling and its application to health-monitoring and prognostics of a pem fuel cell, Int. J. of Prognostics and Health Management 5.
[50] F. M. Collette, F. Thominette, H. Mendil-Jakani, G. Gebel, Structure and transport properties of solution-cast nafionÂő membranes subjected to hygrothermal aging, J. of Membrane Science 435 (2013) 242 – 252.
[51] A. Bose, P. Babburi, R. Kumar, D. Myers, J. Mawdsley, J. Mil-

huff, Performance of individual cells in polymer electrolyte membrane fuel cell stack under-load cycling conditions, J. of Power Sources 243 (2013) 964 – 972.

[52] I. Radev, K. Koutzarov, E. Lefterova, G. Tsotridis, Influence of failure modes on PEFC stack and single cell performance and durability, Int. J. of Hydrogen Energy 38 (17) (2013) 7133 – 7139.

[53] F. Research, Ieee phm data challenge 2014 (2014).
URL `http://eng.fclab.fr/ieee-phm-2014-data-challenge/`

[54] I. Sobol, S. Tarantola, D. Gatelli, S. Kucherenko, W. Mauntz, Estimating the approximation error when fixing unessential factors in global sensitivity analysis, Reliability Eng. & System Safety 92 (7) (2007) 957 – 960.

[55] F. Cannavo, Sensitivity analysis for volcanic source modeling quality assessment and model selection, Computers and Geosciences 44 (2012) 52 – 59.

[56] M. Lamboni, B. Iooss, A.-L. Popelin, F. Gamboa, Derivative-based global sensitivity measures: General links with sobol indices and numerical tests, Mathematics and Computers in Simulation 87 (2013) 45 – 54.

[57] M. Jouin, R. Gouriveau, D. Hissel, M.-C. Péra, N. Zerhouni, Prognostics of pem fuel cells under a combined heat and power profile., in: 15th IFAC/IEEE/IFIP/IFORS Symposium Information Control Problems in Manufacturing, INCOM'15., OTTAWA, CANADA, 2015, pp. 1–6.

[58] M. Jouin, R. Gouriveau, D. Hissel, M.-C. Péra, N. Zerhouni, Pemfc aging modeling for prognostics and health assessment., in: 9th Int. Symposium on Fault Detection, Supervision & Safety of Technical Processes, SAFEPROCESS'15., PARIS, 2015, pp. 1–6.